ELSEVIER

Journal of Hazardous Materials B101 (2003) 109–122

Journal of Hazardous Materials

www.elsevier.com/locate/jhazmat

Enhanced removal of DNAPL trapped in porous media using simultaneous injection of cosolvent with air: influencing factors and removal mechanisms

Seung-Woo Jeong*, A. Lynn Wood, Tony R. Lee

US Environmental Protection Agency, Office of Research and Development, National Risk Management Research Laboratory, Subsurface Protection and Remediation Division, 919 Kerr Research Dr., Ada, OK 74820, USA

Received 23 May 2002; received in revised form 25 October 2002; accepted 28 October 2002

Abstract

Factors influencing dense non-aqueous phase liquid (DNAPL) removal by concurrent injection of cosolvent and air were evaluated using micromodels and visualization techniques. Cosolvent (ethanol/water) was injected simultaneously with air into glass micromodels containing residual perchloroethylene (PCE). Impacts of the air flow rates and PCE solubility in the remedial fluid on PCE removal processes were examined. Although two major processes, immiscible displacement and dissolution, may contribute PCE removal from porous media during cosolvent-air (CA) flooding, PCE displacement occurred only in the initial flooding period and was independent of the air flow rate and ethanol content. However, faster airflow through the porous medium improved remedial fluid distribution and dynamics and resulted in enhanced dissolution of the DNAPL. Dissolution rates were directly related to PCE solubility in the remedial fluid. Enhanced contact between cosolvent and DNAPL during CA flooding was observed in a non-homogeneous micromodel with random flow paths.
Published by Elsevier Science B.V.

Keywords: DNAPL; Cosolvent; Dissolution; Immiscible displacement; Remediation; Porous media

1. Introduction

Groundwater contamination by dense non-aqueous phase liquids (DNAPLs) presents a formidable challenge. Two representative characteristics of DNAPL are low water solubility and high toxicity. Because DNAPL migrate downward until low permeability strata is encountered, discontinuous immobile blobs and DNAPL pools can be formed, resulting in

* Corresponding author. Present address: Korea Environment Institute, Seoul 122-706, South Korea.
Tel.: +82-11-9075-3595; fax: +82-2-380-7744.
E-mail addresses: superjeong@yahoo.com (S.-W. Jeong), wood.lynn@epa.gov (A. Lynn Wood).

0304-3894/$ – see front matter. Published by Elsevier Science B.V.
PII: S0304-3894(02)00313-8

local saturations from 1 to 70–80% [1]. Because conventional pump-and-treat remediation efforts have been ineffective, several in situ flooding methods using cosolvents and surfactants have been suggested and evaluated for enhanced DNAPL source removal [2,3]. These methods involve the injection of remedial fluids or chemicals into the DNAPL-contaminated formations in order to enhance either dissolution or mobilization of DNAPL. Because of the risk of uncontrolled DNAPL migration during mobilization, enhanced dissolution is often the preferred removal approach.

A major obstacle for using in situ flushing may be low sweep efficiency of remedial fluids in porous media, especially for heterogeneous systems. Only partial DNAPL dissolution by cosolvent has been observed even in small-scale flooding systems [4]. Recently, simultaneous injection of cosolvent with air, i.e. cosolvent-air (CA) flooding, has been suggested to enhance sweep efficiency of cosolvent flooding. Injected air phase tends to flow through preferential flow paths in a porous medium [5]. Air flowing through the preferential flow paths may displace cosolvent from these paths into less permeable paths. The CA flood utilizes the preferential flow of air in porous media for distribution of remedial fluids. Flow channeling of gas in a saturated porous medium facilitated fluid distribution and dynamics of the cosolvent solution, resulting in enhanced dissolution of residual perchloroethylene (PCE) [6].

Three PCE removal processes occur during CA floods: (1) displacement (injected air displaces water and PCE phases through immiscible displacement mechanisms); (2) volatilization (PCE volatiles into the air phase); (3) dissolution (cosolvent which was injected with air dissolves PCE trapped in the porous medium). Understanding relative importance of the removal processes in the CA flood may provide a means to help design effective CA floods. The objectives of this study were to elucidate the DNAPL removal mechanisms of the CA flood by evaluating the effects of air flow rate and DNAPL solubility, and to visually document DNAPL removal mechanisms at a pore-scale. Impacts of the air flow and PCE solubility were evaluated by changing air flow rate and ethanol content, respectively. Pore-scale visualization of CA and cosolvent flooding in a non-homogeneous porous medium improve our understanding of DNAPL removal mechanisms.

2. Materials and methods

2.1. Micromodel production

The micromodels used in this study were made of etched glass. The models were fabricated at US EPA's Robert S. Kerr Environmental Research Center, Ada, OK, using a photo-fabrication technique modified from the fabrication methods discussed by Buckley [7]. Two different patterns of pore networks were created using CorelDraw software. The generated drawing of the pore network was used as a mask on the exposed copper surface of glass mirror stock. The network patterns were etched into the glass by hydrofluoric acid. Etched lines act as the void space through which fluids flow, while grains of soil are simulated with unetched portions. Mirror images of the pattern were prepared and fused together to create a micromodel. The model shown in Fig. 1 has an irregular flowpath pattern.

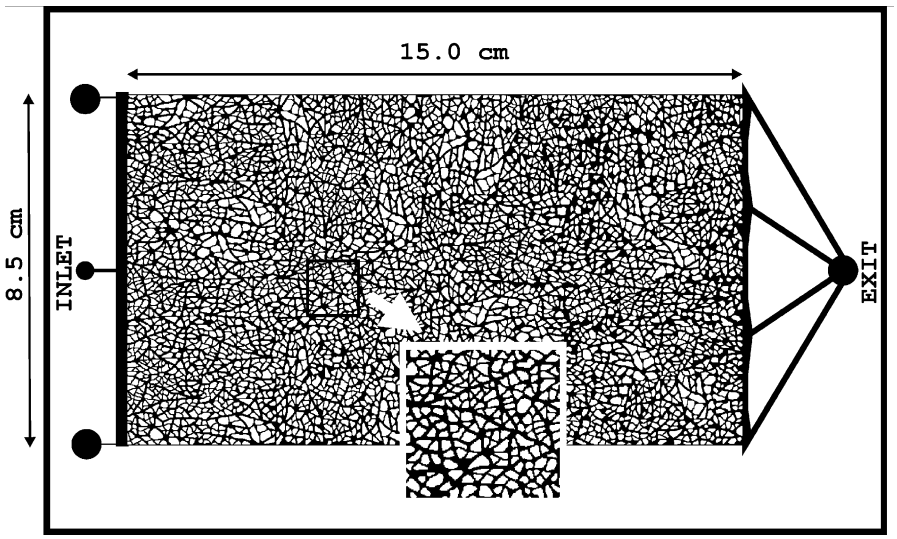

Fig. 1. Micromodel configuration: a random flow pattern.

Behavior in a homogeneous network (regular flowpath pattern) was presented in Jeong et al. [6]. The irregular pattern consists of relatively uniform distributions of anglular glass grains of varying shapes and sizes. The irregular flowpath model has a local microscopic heterogeneity due to the variation in particle sizes and configuration. Some larger flow channels are present parallel to the flow direction. The larger channels may act as preferential flow paths. The properties of the micromodels are shown in Table 1. The depth of the micromodels was measured as 110 μm.

2.2. Experimental apparatus and methods

The same experimental apparatus reported in Jeong et al. [6] was used for this study. PCE was chosen as the DNAPL for this study. The PCE (>99.9%, Sigma) was dyed with 0.5 g/l of Oil-Red-O (Fisher Scientific). To investigate the effect of cosolvent concentration on PCE

Table 1
Micromodel properties

Micromodels	Permeability[a] (cm^2)	Effective permeability[b] (cm^2)	Porosity[c]	Pore volume[d] (ml)
Homogeneous flow pattern [6]	2.43×10^{-7}	3.58×10^{-8}	0.64	0.95
Random flow pattern, Fig. 1	2.09×10^{-5}	7.77×10^{-8}	0.41	0.87

[a] Obtained from data sets of given flow rate and measured pressure response.
[b] At residual PCE saturated conditions.
[c] Ratio of void area to total area.
[d] Obtained by weight difference between water saturated and dried micromodel.

Table 2
Fluid properties

Fluid	Density[a] (mg/l)	Viscosity[a,b] (cP)	PCE[a,c] solubility (mg/l)	Interfacial tension with red dyed PCE[a,c,d] (dyn/cm)
PCE	1.627[a]	0.84[e]		
Water	1.001	0.91 ± 0.002	150	39.10 ± 0.40
50% (v/v) ethanol	0.935	2.38 ± 0.01	4,970	5.86 ± 0.06
70% (v/v) ethanol	0.895	2.33 ± 0.01	49,100	2.71 ± 0.06
90% (v/v) ethanol	0.853	1.86 ± 0.01	214,000	0.77 ± 0.03

[a] Room temperature (22 ± 1 °C).
[b] Ubbelohde calibrated viscometer, ASTM D445.
[c] 0.5 g Oil-Red-O/L PCE.
[d] Drop volume method (measured after saturated with red-dyed PCE).
[e] [11].

removal, three cosolvent solutions were used: 50% ethanol/50% water, 70% ethanol/30% water, and 90% ethanol/10% water, by volume basis. Selected properties of fluids used in this study are given in Table 2.

Density was determined by using a pycnometer (Kimble Glass Inc.). Viscosity was measured by a Cannon®—Ubbelohde viscometer and determined according to the procedures of ASTM D 445. Interfacial tensions between the PCE and aqueous solutions were measured by the drop volume method [8]. Solubility and interfacial tension were measured after each solution was fully saturated with the dyed PCE. Details of measurement methods for the properties of fluids were described in Jeong et al. [9].

The micromodels were vertically placed and saturated with water. PCE was introduced to the micromodel until breakthrough at the outlet was observed. The micromodels were then horizontally laid and residual PCE saturation was obtained by flushing the micromodel with water until mobilization ceased. The average PCE saturation was 0.32. Micromodels were horizontally laid during flooding. In the homogeneous model experiments, remedial aqueous phase fluids were injected at a rate of 0.02 ml/min (Darcy velocity = 0.96 m per day). Air was injected at a flowrate of 0.04 and 0.1 ml/min, respectively. In the random flow pattern model experiments, the cosolvent injection flow rate and air injection rate were 0.017 and 0.086 ml/min, respectively, which resulted in the same Darcy velocities as the homogeneous model experiments. Air and cosolvent were injected into the inlet tube at the same time [6]. Therefore, alternating slugs of cosolvent and air were formed inside the inlet tube. Pressure gradients during flooding were monitored with a pressure transducer (Cole Parmer Model J-7354). The pressure difference between inlet and outlet was measured and stored in a computer containing data logging software (LabView® v.6.0, National Instruments Inc.).

PCE saturation is the ratio of trapped PCE volume to pore volume. Results were expressed as a normalized PCE saturation, the ratio of the PCE saturation (S_{PCE}) after flooding to the initial S_{PCE} before flooding. PCE saturation can be determined by the ratio of the total area of red colored PCE to the total void area. Image analysis software (Optimas v.6.5, Media Cybernetics Inc.) allowed measurement of the total area occupied by dyed DNAPL. Details of the quantification method are described in Jeong et al. [6].

3. Results and discussion

3.1. PCE removal by volatilization

Previous work showed negligible volatilization of PCE after displacement of 40 PV of air [6]. This study approximately calculated the portion of the residual PCE volatilized during the CA floods. Mass balance of PCE between fluid phases can be described by Eq. (1) [10]:

$$V_a \frac{dC_a}{dt} = k_g A(HC_w - C_a) - QC_a \quad (1)$$

To obtain the maximum PCE saturation that can be removed by volatilization, the system was treated as steady state and the PCE solubility in the cosolvent was used as the PCE concentration in the aqueous phase, C_w. The air phase concentration of PCE, C_a, was calculated and use to estimate the volume of PCE removed by volatilization. Details of the calculation and nomenclatures are shown in Table 3. Based on this analysis, approximately 1.2% of the initial residual PCE was volatilized by air during CA flood under experimental conditions descried in Table 3. Therefore, the PCE volume removed by volatilization was ignored in the assessment of results for this study.

3.2. Effect of air flow rate on PCE and cosolvent displacements

Fig. 2 shows the effect of air flow rate during CA flooding on PCE removal. Cosolvent:air injection ratios of 1:5 and 1:2 were evaluated in the homogeneous micromodel. Ethanol content of the cosolvent solutions remained constant at 70% (v/v). All replicate data of CA floods and cosolvent floods are plotted in Fig. 2. Data of cosolvent + air 0.10 ml/min are obtained from Jeong et al. [6] and shown with range bars. PCE desaturation patterns as if a function of total pore volume injected were similar for the two air flow rates (Fig. 2(a)). However, more efficient PCE removal was observed at the higher flow (cosolvent:air injection ratio of 1:5), if comparisons are made on the basis of equivalent volumes of injected cosolvent (Fig. 2(b)).

The results of these experiments were also plotted in one-dimensional graphs to show changes in PCE distribution within the pore network (Fig. 3). The pore network of the homogeneous model was divided into 10 horizontal regions which were parallel to the flow direction, as shown in Fig. 3(a). PCE saturation within each region was determined by image analysis. Fig. 3(b)–(d) show changes in PCE saturations during flooding with cosolvent:air injection ratios of 1:0, 1:2, and 1:5, respectively. Distinct differences were observed in the PCE saturation distribution between CA floods and cosolvent flood. Replicate experiments for the two different flooding techniques showed different removal patterns (see Fig. 3). In cosolvent flood, dissolution of residual PCE occurred primarily in the interval between $y = 0$ and $y = 0.5$ (see Fig. 3(b)). The results suggest poor contact between residual PCE and injected cosolvent in the region defined by $y = 0.6$ to $y = 1.0$. Poor contact at the region defined by $y = 0.6$ to $y = 1.0$ may be related to the non-uniform distribution of DNAPL blobs in the micromodel. As illustrated in Fig. 3(c) and (d), PCE removal was relatively uniform when air was injected with the cosolvent. PCE removal over the interval $y = 0.6$ to $y = 1.0$ was enhanced with increased air flow (Fig. 3(d)). This enhancement

Table 3
PCE volatilization into the air phase; nomenclatures for Eq. (1)

Symbols	Parameters	Applied or obtained values	Remark
Sh	Sherwood number	$Sh = 10^{-4.71}\, Pe^{0.84} d_0^{1.71}\, H^{-0.61}$	[10]
D_g (cm^2/s)	Diffusion coefficient (PCE in air)	0.082	[10]
d_m or d_{50} (cm)	Grain diameter	0.0758	Equivalent diameter to grain volume
D_0	Normalized mean particle size (d_{50}/d_m)	1	Homogeneous network pattern
v_g (cm/s)	Gas velocity	0.00868	
Pe	Peclet number	0.00802	$Pe = v_g d_{50}/D_g$
H	Henry's law constant	0.667	[10]
$k_g\, a$ (per day)	Estimated mass transfer rate coefficient	0.535	Equals to $k_g A/V_a$ (k_g: mass transfer coefficient; A: surface area; V_a: system volume)
C_w (g/cm^3)	PCE concentration in the aqueous phase	0.0491	PCE solubility in 70% ethanol
Q (cm^3/s)	Air flow rate	0.00167	Flood period = 316 min (33 PV)
C_a (g/cm^3)	PCE concentration in the air	0.00020	
Calculated results (cm^3)	Removed PCE volume by volatilization	0.00379	
	Portion of PCE removed by volatilization	0.012 (1.2% of the residual PCE)	Based on average initial PCE volume = 0.304 cm^3

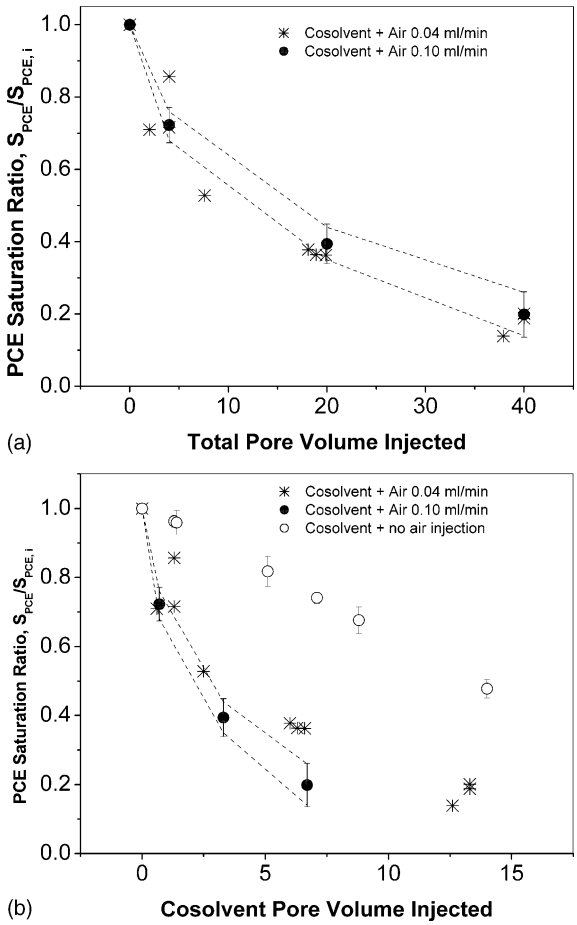

Fig. 2. Normalized PCE saturations measured in homogeneous micromodel during cosolvent-air (CA) flooding, 70% (v/v) ethanol was injected at a rate of 0.02 ml/min. Air was concurrently injected at a rate of 0.04 and 0.10 ml/min, respectively: (a) $S_{PCE,i}$ is the initial PCE saturation. Results are shown as a function of total pore volume of fluids injected; (b) Results are shown on the basis of equivalent volumes of injected cosolvent. Data of cosolvent + air 0.10 ml/min are obtained from Jeong et al [6].

may be a result of improved PCE displacement by air or better PCE dissolution as a result of enhanced contact between cosolvent and PCE. Therefore, more analysis is required to understand which removal mechanism contributes to the higher PCE removal efficiency.

Displacing fluid can flow through pore necks if its pressure becomes greater than the capillary pressure of the pore neck. Thus, pressures and gas saturations were monitored within the micromodel during CA flooding. Fig. 4 shows both pressure response and PCE removal efficiency and Fig. 5 shows gas saturations during CA flooding. High pressures were observed during the initial period of flooding. These initial pressure spikes occurred before breakthrough of the remedial fluids. Direct PCE displacement by air occurred only during the initial high pressure conditions. After remedial fluid breakthrough, the pressure

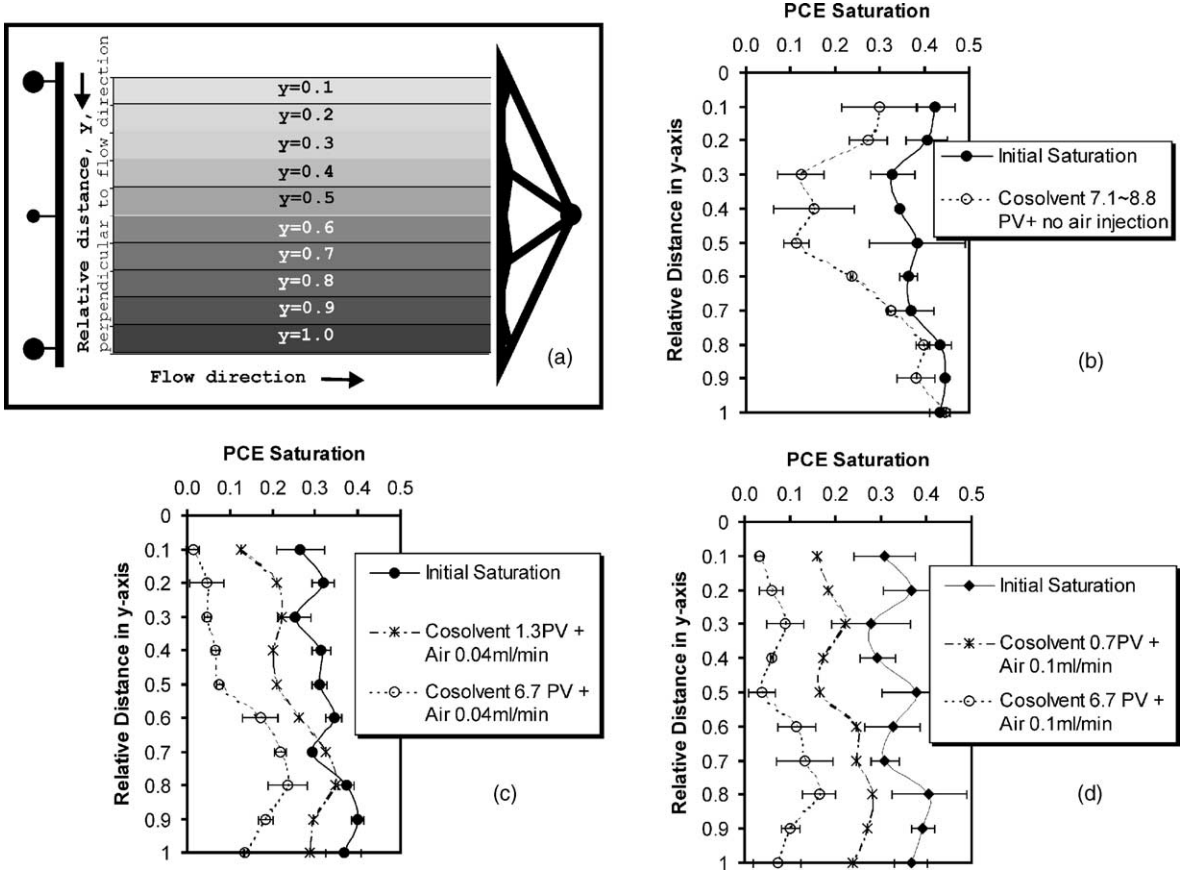

Fig. 3. (a) Dividing the homogenous pattern micromodel into 10 horizontal regions, parallel to flow direction; PCE saturations were measured in each horizontal region (from $y = 0.1$ to $y = 1.0$), before and after flooding; data ranges of replicate experiments are shown with error bars; (b) PCE saturation distribution in flooding with cosolvent 0.02 ml/min and no air injection; (c) PCE saturation distribution in flooding with cosolvent 0.02 ml/min and air 0.04 ml/min; (d) PCE saturation distribution in flooding with cosolvent 0.02 ml/min and air 0.10 ml/min.

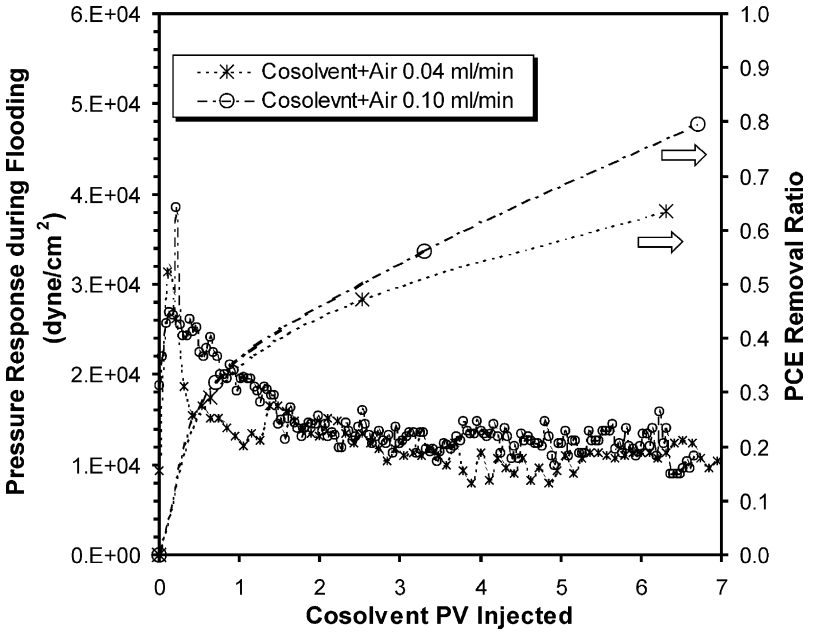

Fig. 4. Changes in pressure and PCE removal efficiency during CA flooding (homogeneous micromodel experiments).

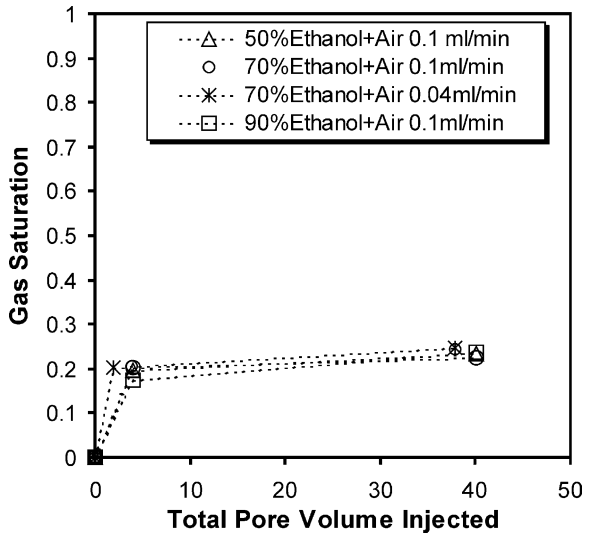

Fig. 5. Changes in gas saturation during CA floods; flow rate of ethanol was 0.02 ml/min (homogeneous model experiments).

decreased and remained relatively stable. Although the initial pressures at the higher air flow rate (0.1 ml/min) were higher than the lower air flow rate (0.04 ml/min), PCE removal during this period was similar for the two flow rates. Thus, PCE displacement by air appeared to be independent of pressure and air flow rate for these experiments.

Gas saturations for all flood conditions are relatively constant and independent of the ethanol content and air flow rate (see Fig. 5). The results imply that preferential flow paths for air are likely similar for all CA flood conditions leading to similar PCE displacement patterns. However, as shown in Fig. 4, difference in the PCE removal efficiency between the two air flow rates became distinct as time elapsed. Therefore, we may attribute the higher PCE removal to enhanced dissolution as a result of improved contact between cosolvent and DNAPL because PCE removal by immiscible displacement by air was not observed as time elapsed [6]. Subsequent to PCE removal by direct displacement, injected air apparently improves distribution of the cosolvent throughout the pore network as a result of flow of air flowing through preferential paths. Cosolvent displaced by air may flow into other flow paths and contact to more PCE. This suggests a direct relationship between air flux and PCE removal by dissolution. Thus, the higher PCE removal rate at the higher air flow rate was most likely due to the efficient dissolution resulting from enhanced contact of cosolvent with PCE.

3.3. Relative importance of PCE removal processes during CA flooding

Two important removal processes, immiscible displacement and dissolution, were mentioned in the earlier section. The results showed that PCE removal by immiscible displacement was independent of the air flow rate and occurred only in the initial period of flooding. This study assessed the importance of dissolution during CA flood. CA floods with different

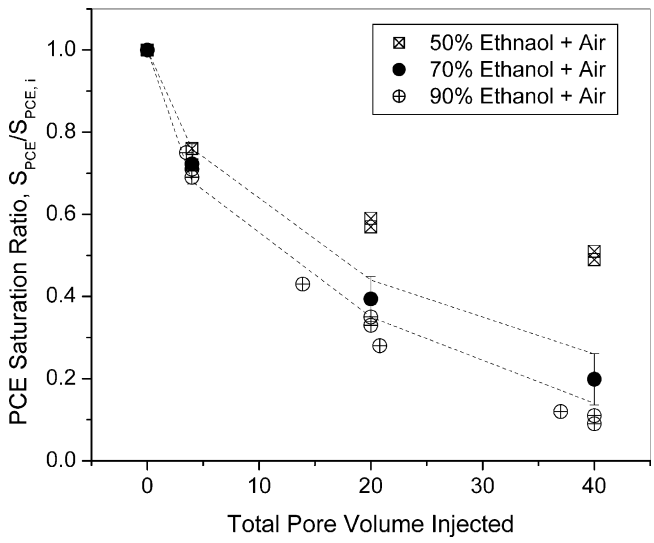

Fig. 6. Normalized PCE saturations measured in the homogeneous micromodel during three different floodings: CA flooding with 50% ethanol, 70% ethanol and 90% ethanol flooding with concurrent air injection.

ethanol contents were conducted to evaluate the effects of cosolvent concentration on PCE removal. The air flow rates were the same, i.e. 0.1 ml/min. As shown in Fig. 6, PCE removal efficiencies during the initial period of the CA floods were similar, implying similar air-induced PCE displacement. However, about 50% removal was obtained with 40 PV flooding of the mixture of 50% ethanol and air, while 80% of the initial PCE saturation was removed after flooding with the same volume of 70% ethanol and even greater removal was observed when the cosolvent contained 90% ethanol. We have to note here that PCE solubility in 50% ethanol is one-tenth of that of 70% ethanol, as shown in Table 1. The results illustrate the importance of contaminant solubility in the remedial fluid for determining the rate of DNAPL dissolution.

3.4. Visualization of PCE removal mechanism in a random flow pattern porous medium

DNAPL removal mechanisms during CA flooding were evaluated in a random flow pattern micromodel which is a more representative of field flow conditions. Figs. 7

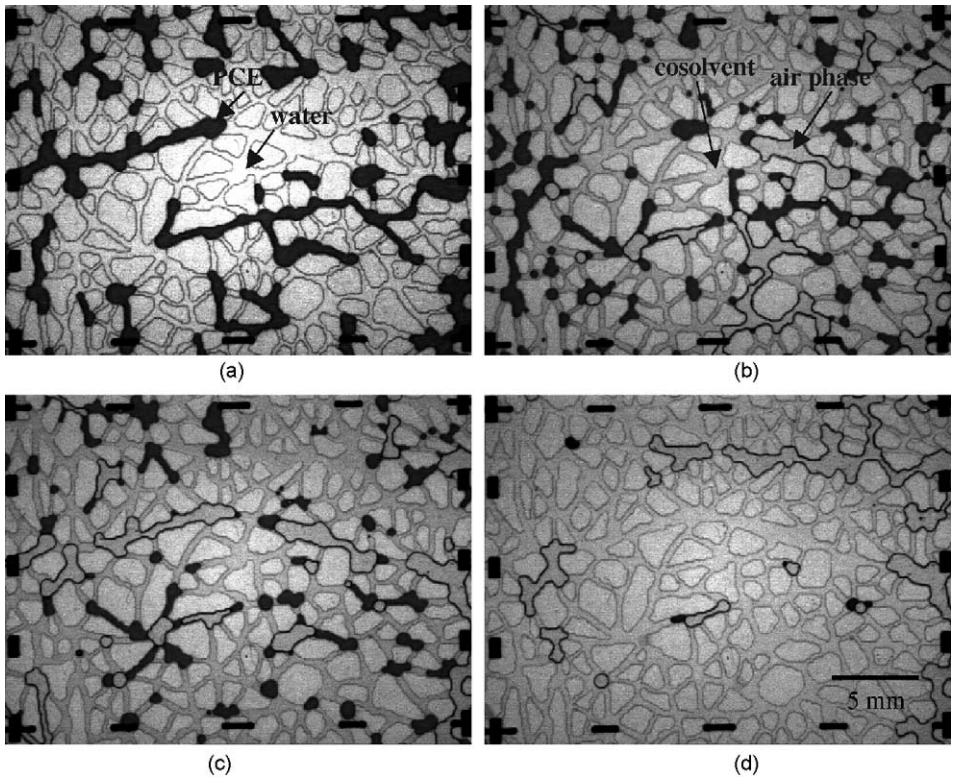

Fig. 7. Microscopic images from a random flow pattern micromdoel during CA flooding, 70% (v/v) ethanol:air = 1:5 (0.017 ml/min:0.086 ml/min): (a) initial image; (b) 40 min elapsed; (c) 3 h elapsed; (d) 8 h elapsed; pore volumes of injected cosolvent were the same with that shown in Fig. 8.

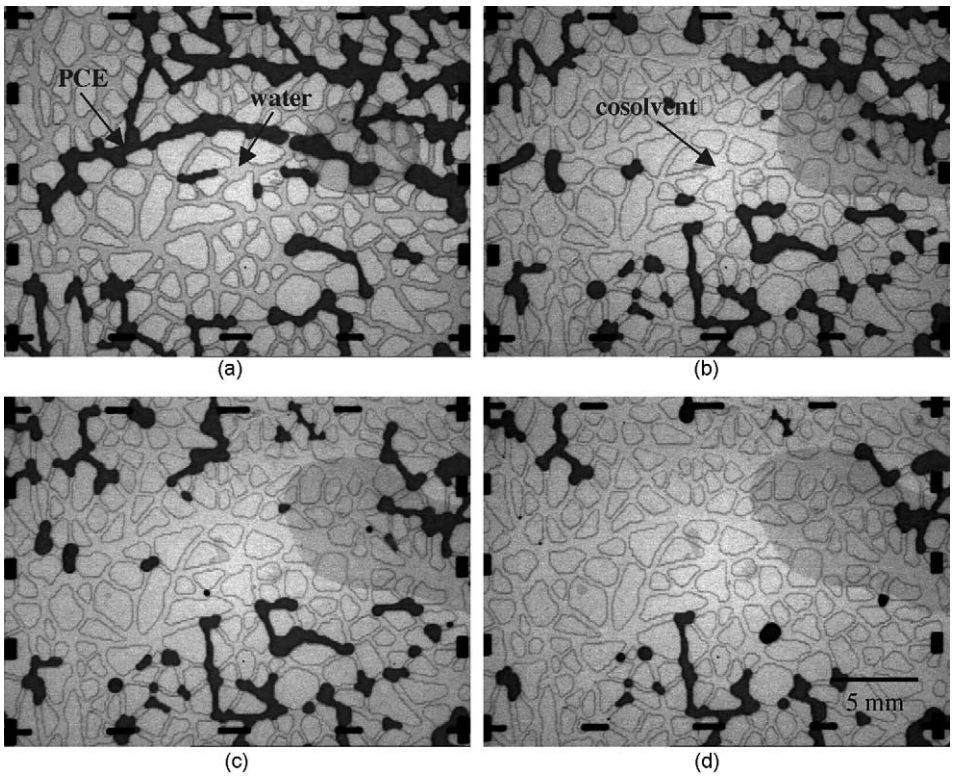

Fig. 8. Microscopic images from a random flow pattern micromodel during cosolvent flooding (70% (v/v) ethanol only): (a) initial image; (b) 40 min elapsed, 0.7 PV; (c) 3 h elapsed, 3.3 PV;(d) 8 h elapsed, 9.7 PV.

and 8 show microscopic images taken from a selected cell during CA flooding and cosolvent flooding, respectively. The flow direction is left to right in the images. The selected cell has a relatively straight flow channel in the direction of the fluid flow. This channel may affect fluid displacement as well as PCE dissolution. Long ganglia of PCE residing in the relatively straight channel was readily removed by either direct displacement by air phase or interfacial tension reduction (see Figs. 7(b) and 8(b)). Fig. 7(b) shows direct PCE displacement by the air which was co-injected with cosolvent. As the cosolvent displaces water, the interfacial tension between the aqueous phase and PCE is reduced (i.e. 39.1 dyn/cm to 2.7 dyn/cm) and the PCE is readily mobilized through the straight channel. Subsequent to this initial displacement, substantial differences are seen in the rates and patterns of DNAPL removal by CA and cosolvent flooding. In cosolvent flooding, cosolvent dissolves PCE in the vicinity of the straight flow path, but PCE removal was relatively slow in other parts of the pore network (Fig. 8(d)). For CA flooding, only a few PCE blobs remained after flushing with an equivalent volume of cosolvent (Fig. 7(d)). As discussed earlier, improved PCE removal observed in the CA flood is apparently the result of enhanced contact between cosolvent and PCE. Based on the observations, injected air flows thorough the

preferential flow paths, displaces PCE residing in these paths, and promotes cosolvent flow in less preferential flow paths. These observations are consistent with results of the previous sections.

4. Summary and conclusions

Glass micromodel experiments were conducted to investigate concurrent injection of co-solvent and air for PCE removal. Two types of glass micromodels were prepared by etching regular flow and random flow patterns on the glass. The experimental set-up consisted of fluid delivery, micromodel, and image analysis systems. This study quantified real-time change in PCE saturation by image analysis. Impacts of air flow rate and PCE solubility on PCE removal processes were studied by changing air flow rate and ethanol content, respectively.

CA flooding with a higher air flow rate resulted in higher PCE removal. The higher removal efficiency was primarily attributed to improved distribution of displaced cosolvent through the pore network and resultant enhanced dissolution. DNAPL mobilization by air was independent of the air flow rate and ethanol content and occurred only in the initial period of flooding.

The results of CA floods with different ethanol contents showed the importance of the PCE solubility during CA flooding. Under the same air flux, the CA flood with 50% ethanol showed a slower removal rate than floods with higher ethanol contents. Dissolution rate was directly related to PCE solubility in the remedial fluid. Micromodel visualization illustrated air flows thorough preferential flow paths, with resultant distribution of cosolvent through less permeable regions.

Acknowledgements

The US Environmental Protection Agency through its Office of Research and Development funded and managed the research described here. This work was performed while Seung-Woo Jeong was a National Research Council Research Associate with the National Risk Management Research Laboratory, Subsurface Remediation and Protection Division Research. This document has not been subjected to Agency review and therefore does not necessarily reflect the views of the Agency, and no official endorsement should be inferred.

References

[1] Interstate Technology and Regulatory Cooperation, Dense non-aqueous phase liquids (DNAPLs): review of emerging characterization and remediation technologies, Interstate Technology and Regulatory Cooperation, http://www.itrcweb.org/DNAPL-1.pdf, 2000.
[2] C.C. West, J.H. Harwell, Environ. Sci. Technol. 26 (1992) 2324.
[3] P.S.C. Rao, M.D. Annable, R.K. Sillan, D. Dai, K. Hatfield, W.D. Graham, A.L. Wood, C.G. Enfield, Water Resour. Res. 33 (1997) 2673.
[4] P.T. Imhoff, S.N. Gleyzer, J.F. McBride, L.A. Vancho, I. Okuda, C.T. Miller, Environ. Sci. Technol. 29 (1995) 1966.

[5] W. Ji, A. Dahmani, D.P. Ahlfeld, J.D. Lin, E.I. Hill, Ground Water Monit. Rem. 13 (1993) 115.
[6] S.-W. Jeong, A.L. Wood, T.R. Lee, Environ. Sci. Technol. 36 (2002) 5238.
[7] J.S. Buckley, in: N.R. Morrow (Ed.), Interfacial Phenomena in Petroleum Recovery, Marcel Dekker, New York, 1991, p. 157.
[8] K. Hool, B. Schuchardt, Meas. Sci. Technol. 3 (1992) 451.
[9] S.-W. Jeong, A.L. Wood, T.R. Lee, J. Hazard. Mater. 95 (2002) 125.
[10] K.-P. Chao, S.K. Ong, A. Protopapas, J. Environ. Eng. 124 (1998) 1054.
[11] D.R. Lide, Properties of Organic Solvents, 2nd ed., CRC Press, Boca Raton, 1996.